Check for updates

Two new photochromic coordination compounds with nonphotochromic ligands and different metal centers†

Jie Liu,[ab] Pei-Xin Li,*[b] Hui-Yi Zeng[b] and Guo-Cong Guo ![ORCID] *[b]

Recent research has demonstrated the effective synthesis of photochromic coordination compounds *via* the assembly of nonphotochromic ligands (electronic donors and acceptors) and a metal center (joint points). To enrich this system, the metal center could be expanded to binuclear or multinuclear, but related studies are rare. Two new photochromic coordination compounds with different metal joint dots were obtained using expanded metal centers. In this work, $[Zn_2(Bpy)_{1.5}(CTA)_4 \cdot 2H_2O]$ (**1**, CTA = crotonic acid, Bpy = 4,4′-bipyridine) and $[Zn_2(Bpy)(CTA)_4]$ (**2**) were synthesized under different pH conditions. Compound **1** features a 1-D chain structure with 4,4′-bipyridine coordinating to mono zinc ions and binuclear Zn units simultaneously. Compound **2** also features a 1-D chain structure, where only the binuclear Zn is bridged by the 4,4′-bipyridine. This work will help to obtain new and promising photochromic compounds with different multinuclear metal centers and high performance.

Introduction

Electron transfer (ET) photochromic materials have attracted great attention due to their increasing applications, such as catalysis and optic, electric, and magnetic switches.[1,2] In past decades, much effort has been concentrated on the traditional families of ET photochromic compounds, such as viologens and polyoxometalates of group VIB metals, due to their merits.[3,4] In recent years, a new class of ET photochromic compounds has been composed of non-photochromic ligands and metal ions through coordination.[5,6] These include metal–organic compounds (MOCs), with various functional materials based on MOCs having been produced with electronic,[7] magnetic,[8] and nonlinear optical[9] characters. Therefore, exploring this type of photochromic species based on MOCs is valuable, and may offer new opportunities to enrich the system and obtain promising photochromic materials.

Few examples of photochromic compounds with non-photochromic ligands have been reported. Their structures usually comprise metal ions and carboxylate groups connected by a coordinated conjugated ligand. Studies have reported the use of conjugated ligands, such as 4,4′-bipy, trigonal 3-connector 2,4,6-tris(4-pyridyl)-1,3,5-triazine, 4,4′-bis(1-imidazolyl)-biphen, 1,3-

di(4-pyridyl)propane, as electron acceptors, carboxylate as the electron donor,[10–12] and electron transfer from the carboxylate to the conjugated ligand *via* through-bond and through-space paths.[13] The corresponding radicals could be trapped at room temperature in a photochromic (conjugated ligand–metal–carboxylate) system by photoexcitation.[14] Therefore, these compounds can be synthesized largely *via* ligand design for photochromic studies and applications. Furthermore, the influence of different metal ions on photosensitivity has been discovered by the Zhang group,[15] whereas photosensitivity is seldom tuned through designing the metal centers in a dinuclear or trinuclear form. Works related to this have so far not been published.

As part of our research into the construction of solid photochromic materials *via* non-photochromic ligand design,[16] we investigated this type of photochromic compounds using multi-metal joint points. We obtained two new Zn(II) coordination compounds, $[Zn_2(Bpy)_{1.5}(CTA)_4 \cdot 2H_2O]$ (**1**, CTA = crotonic acid, Bpy = 4,4′-bipyridine) and $[Zn_2(Bpy)(CTA)_4]$ (**2**). These were synthesized in different pH environments and were sensitive to UV light. Controlling the environments is a useful approach to building various fascinating multimetal clusters[17] as the joint point of different photochromic compounds. Here, their synthetic crystal structure, and photochromic and photoluminescence properties, are presented.

Experimental section

Materials and instruments

Analytical reagent grade $3Zn(OH)_2 \cdot 2ZnCO_3$, crotonic acid, acetonitrile, and 4,4′-bipy were purchased from commercial

[a]Fuzhou University, Fuzhou, Fujian 350108, PR China

[b]State Key Laboratory of Structural Chemistry, Fujian Institute of Research on the Structure of Matter, Chinese Academy of Sciences, Fujian, Fuzhou, 350002, PR China. E-mail: gcguo@fjirsm.ac.cn; lipeixin@fjirsm.ac.cn

sources. Water was deionized and distilled before use. Elemental analyses for C, H, and N were measured on an Elementar Vario EL III microanalyzer. A PLSSXE300C 300 W xenon lamp system equipped with an IR filter was used to prepare colored samples for UV-visible (UV-Vis), powder X-ray diffraction (PXRD), and electron spin resonance (ESR) studies, with a distance between the samples and the xenon lamp of around 40 cm. UV-visible spectra were recorded using a PerkinElmer Lambda 900 UV/Vis/near-IR spectrophotometer equipped with an integrating sphere in the wavelength range 200–1000 nm. $BaSO_4$ plates were used as a reference (100% reflection), on which the sample was coated as a finely ground powder. PXRD patterns were collected with a Rigaku MiniFlex II diffractometer powered at 30 kV and 15 mA for Cu-Kα radiation ($\lambda = 1.54056$ Å) in the range 5–50° at room temperature. Simulated PXRD patterns were achieved using Mercury Version 1.4 software (http://www.ccdc.cam.ac.uk/products/mercury/) and reported single-crystal X-ray diffraction data. Thermogravimetric analysis (TGA) experiments were performed on an NETZSCH STA 449F3 Jupiter thermogravimetric analyzer under N_2 with the sample heated in an Al_2O_3 crucible at a rate of 15 K min^{-1}. ESR spectra were recorded at the X-band frequency (9.867 GHz) on a Bruker ELEXSYS E500 spectrometer. *In situ* photoluminescence (PL) determination was conducted on a single-grating Edinburgh FL920 fluorescence spectrometer equipped with a 450 W Xe lamp and a R928P PMT detector.

Synthesis of compounds

[Zn$_2$(Bpy)$_{1.5}$(CTA)$_4$·2H$_2$O] (1). A mixture of 4,4′-bipy (0.2 mmol), CTA (0.8 mmol), $3Zn(OH)_2$·$2ZnCO_3$ (0.1 mmol), and H_2O (4.5 mL) (pH ≈ 6.2) was sealed in a poly(tetrafluoro-ethylene)-lined stainless steel container under autogenous pressure, heated to 100 °C for 3 days, and then allowed to cool to room temperature. Colorless block-shaped crystals suitable for X-ray analysis were obtained. Yield: 50% (based on Zn) for **1**, anal. calcd for $C_{31}H_{36}N_3O_{10}Zn_2$: C, 50.20; H, 4.89; N, 5.66%. Found: C, 50.00; H, 4.84; N, 5.41%.

[Zn$_2$(Bpy)(CTA)$_4$] (2). A mixture of 4,4′-bipy (0.2 mmol), CTA (0.8 mmol), $3Zn(OH)_2$·$2ZnCO_3$ (0.1 mmol), H_2O (1.5 mL), and CH_3CN (3 mL) (pH ≈ 5.8) was sealed in a poly(tetrafluoro-ethylene)-lined stainless steel container under autogenous pressure, heated to 100 °C for 3 days, and then allowed to cool to room temperature. Colorless block-shaped crystals suitable for X-ray analysis were obtained. Yield: 80% (based on Zn) for **2**, anal. calcd for $C_{26}H_{28}N_2O_8Zn_2$: C, 49.78; H, 4.49; N, 4.46%. Found: C, 49.44; H, 4.47; N, 4.48%.

Crystal structure determination

Single-crystal X-ray diffraction measurements of **1** and **2** were performed on a Rigaku Pilatus CCD, which was all equipped with Mo Kα radiation ($\lambda = 0.71073$ Å), using the ω-scan technique to collect intensity data sets. Primitive structures were solved using direct methods and reduced using CrystalClear software.[18] All hydrogen atoms were obtained by Fourier synthesis and using a full-matrix least-squares refinement on F^2 to obtain the final structure. All non-hydrogen atoms used

Table 1 Crystal data and structural refinements for compounds **1** and **2**

Complex	1	2
Empirical formula	$C_{31}H_{36}N_3O_{10}Zn_2$	$C_{26}H_{28}N_2O_8Zn_2$
M_r (g mol^{-1})	741.37	627.28
Crystal system	Triclinic	Triclinic
Space group	$P\bar{1}$	$P\bar{1}$
a (Å)	7.7660(3)	7.8730(4)
b (Å)	11.3054(5)	9.2372(5)
c (Å)	19.0411(7)	9.9610(5)
α (°)	99.745(3)	72.004(5)
β (°)	91.795(3)	76.996(4)
γ (°)	91.783(3)	76.160(4)
V (Å^3)	1645.72(11)	659.95(6)
Z	2	2
D_c/g cm^{-3}	1.496	1.578
μ/mm^{-1}	1.517	1.869
$F(000)$	766	322
Reflections collected	15 047	6107
Unique reflections	7997	3260
GOF	1.032	1.020
R_1^a [$I > 2\sigma(I)$]	0.0361	0.0434
wR_2^b (all data)	0.1832	0.1167
CCDC no.	1542261	1542260

^{a} $R_1 = \sum(F_o - F_c)/\sum F_o$. ^{b} $wR_2 = [\sum w(F_o^2 - F_c^2)^2/\sum w(F_o^2)^2]^{1/2}$.

anisotropic refinement and hydrogen atoms were generated on C and N atoms using the theory of hydrogenation method and refined using the O–H distance restrained to a target value of 0.85 Å, the H···H distance restrained to 1.34 Å, and $U_{iso(H)} = 1.5U_{eq(O)}$. All calculations were performed using the Siemens SHELXTL version 5 crystallographic software package.[19] Relevant crystal data, structural refinement results, and selected bond distances and angles for **1** and **2** are listed in Tables 1 and S1,† respectively.

Entries CCDC-1542261 and CCDC-1542260 contain supplementary crystallographic data for **1** and **2**.†

Results and discussion

Crystal structure and characterization

Compounds **1** and **2** were crystallized in the triclinic $P\bar{1}$ space group, as identified using single-crystal and powder XRD techniques (Fig. S1†). The thermogravimetric analysis (TGA) curves (Fig. S2†) showed that **1** had a weight loss of 4.40% in the temperature range 30–120 °C, corresponding to the loss of two free water molecules (calcd, 4.85%). Continued heating led to decomposition of the framework at ~172 °C. TGA data for **2** showed a stable platform in the temperature range 30–230 °C, while continuous heating led to the breakdown of the framework.

Crystal structure

For **1**, there were two crystallographically independent Zn(ɪɪ) centers, one and a half 4,4′-bipy ligands, four CTA ligands and two free water molecules in the asymmetric unit (Fig. 1a). One Zn atom (Zn1) was four-coordinate with two nitrogen atoms (Zn1–N, 2.0527–2.0763 Å) from two 4,4′-bipy ligands and two
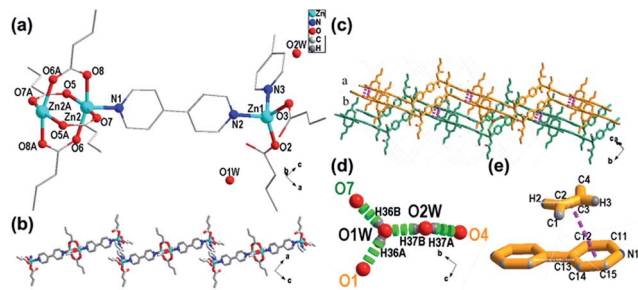
Fig. 1 Structure of compound 1: (a) asymmetric unit; symmetry codes: ① −1 − x, 1 − y, −z; ② 1 − x, 3 − y, 1 − z. (b) View of 1-D trapezoidal chain structure along b axis; and (c) 3-D packing structure. Hydrogen bonds ((d), green dashed line) and π···π stacking interaction ((e), pink dashed line) are shown.

oxygen atoms (Zn1–O, 1.9292–1.9756 Å) from two CTA ligands, while the Zn2 atom had a rectangular pyramidal coordination sphere, with four oxygen atoms from four CTA ligands (Zn2–O, 2.0191–2.1162 Å) and one nitrogen atom (Zn2–N, 2.0402 Å) from one 4,4′-bipy ligand. Two Zn2 atoms were bridged by carboxylate groups to form binuclear Zn units with a neighboring Zn···Zn separation of 2.9308(5) Å. The 4,4′-bipy ligands were alternately connected with the binuclear Zn units and Zn1 ion. Stair-like 1D chain structures were formed along b axis in 1 (Fig. 1b). The center-to-center distance between the nearest pyridinium ring and double bond of CTA was 3.5230(1) Å and the angle between the pyridinium plane and CTA plane was 11.91(15)° (Fig. 1e). Accordingly, π···π stacking interactions between the pyridinium ring and CTA were not overlooked. As shown in Fig. 1c, the distance between two different adjacent chains (green and orange chains) was about 4.0034(59) Å (O1···C5, O1 in the green chain, C5 in the orange chain). Consequently, they were connected by water molecules through O(1w)–H(36A)··· O(1), O(1w)–H(36B)···O(7), O(2w)–H(37A)···O(4), and O(2w)–H(37B)···O(1w). The hydrogen bond distances and angles[20] are summarized in Table 2. Chains connected via π···π interactions[21–23] were further linked though hydrogen bonding interactions with water molecules, leading to a 3D supramolecular structure (Fig. 1c).

Only one crystallographically independent Zn(II) center (Fig. 2a) existed, with two CTA ligands and one 4,4′-bipy ligand in an asymmetric unit of compound 2. Each Zn(II) center was coordinated by one nitrogen atom (Zn–N, 2.0389) from the 4,4′-bipy ligand and four oxygen atoms (Zn–O, 2.0335–2.0708) from four different CTA ligands. Every two Zn atoms were bridged by carboxylate groups to form a classic dinuclear unit with a neighboring Zn···Zn separation of 2.8996(1) Å (Fig. 2a). These

classic dinuclear units were further linked to a 4,4′-bipy ligand, forming a 1-D –[Zn$_2$(CTA)$_4$-Bpy-Zn$_2$(CTA)$_4$]$_n$– linear chain structure along the a axis (Fig. 2b). In compound 2, 4,4′-bipy ligands act as screws to connect units. The nearest distance of two neighboring chains (C3···C14) was about 3.3239(36) Å, and the center-to-center π···π distance (pink dashed line shown in Fig. 2d) between the pyridinium ring and CTA double bond was 3.3624(2) Å, with these two planes forming an angle of 6.20(4)° (Fig. 2d). Structural analysis of 2 revealed the presence of a π···π stacking interaction between the pyridinium ring in 4,4′-bipy and the double bond in CTA from different chains. Finally, these chains formed a 3-D crystal structure along the b axis (Fig. 2c).

As we proposed previously, the coordination assembly of one conjugated ligand (as an electron acceptor), one ligand with groups containing lone pairs of electrons (as an electron donor), and a metal center could obtain photochromic compounds.[24] Compounds 1 and 2 were not exceptions, showing electron transfer behavior under photoirradiation.

Photochromic properties

As shown in Fig. 3, bulk colorless crystals of 1 turned light purple after irradiation with a 300 W Xe lamp under ambient conditions. The photoresponse range was ∼330–370 nm for 1, with an optimal wavelength of about 340 nm. The UV-Vis absorption spectrum showed that two new broad absorption
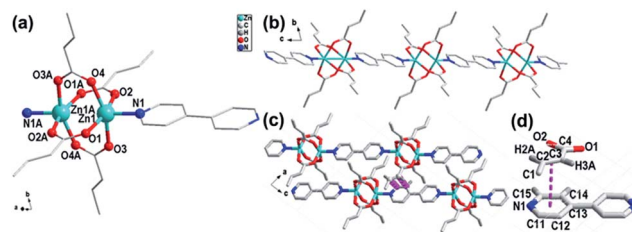

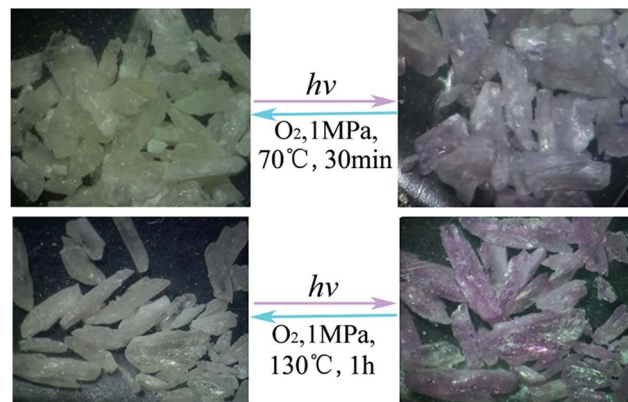Fig. 2 Structure of compound 2: (a) asymmetric unit; symmetry codes: ① 1 − x, 2 − y, −z; ② 2 − x, 2 − y, 1 − z. (b) 1-D linear chain structure along a axis; (c) packing structure viewed along b axis; and (d) π···π stacking interaction between a pyridinium ring and the CTA double bond.

Table 2 Hydrogen bond distances (Å) and angles (°) in compound 1

Hydrogen bond	Distance (Å)	Hydrogen bonds	Angles (°)
O4–H37A	2.06(24)	H36A–O1W···H37B	130.63(1861)
O1W–H37B	2.06(33)	H36B–O1W···H37B	119.96(1074)
O7–H37B	2.18(156)	H37B–O2W–H37A	109.50(383)
O1–H36A	2.11(314)	H36A–O1W–H36B	108.41(3467)

Fig. 3 Photochromism of 1 (top) and 2 (bottom).

bands centered at ~385 and 562 nm emerged and gradually grew larger with increasing irradiation time (Fig. 4). ESR indicated that a symmetric single-line radical signal with a g value of 2.0038 emerged (Fig. 5) during the photochromic process, which was very close to that of a free electron (2.0023). This demonstrated that the photochromic process of **1** originated from photo-induced free radical generation and was an electron-transfer process. The photoproduct of **1**, **1P**, could be bleached slowly in the dark under ambient conditions (Fig. S4†), but was also easily bleached by annealing under O_2 (1 MPa) at 70 °C for 30 min. These photoinduced coloration–decoloration processes were reversible, which demonstrated that **1** had photochromism characteristics. Compound **2** also underwent a color change from colorless to purple after photoirradiation using the same energy xenon lamp under ambient conditions (Fig. 3). The photoresponse range was ~330–370 nm for **2**, with an optimal wavelength of about 340 nm. The UV-Vis absorption spectrum showed two new broad absorption bands centered at ~385 and 572 nm, which grew larger with increasing irradiation time (Fig. 4). An ESR study indicated a symmetric single-line radical signal with a g value of 2.0038 emerged (Fig. 5) in the photochromic process, and the generation of radicals. The photoproduct of **2**, **2P**, could be bleached slowly in the dark under ambient conditions (Fig. S4†), but was also
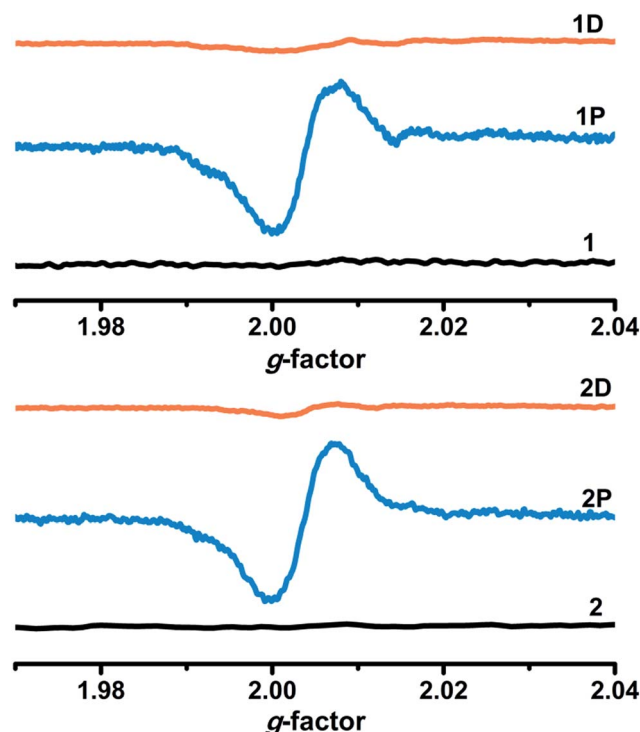

Fig. 5 ESR spectra of **1** and **2** before and after irradiation (**1P**, **2P**) and decolored (**1D**, **2D**) under ambient conditions.
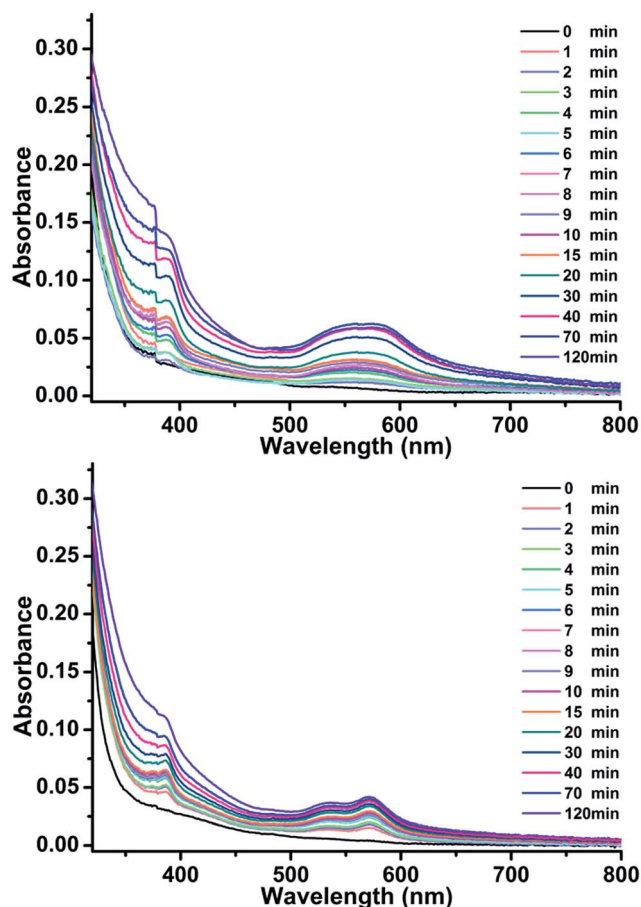
bleached after annealing at 130 °C for 2 h in air or after annealing at 130 °C under O_2 (1 MPa) for 1 h (Fig. S6†).

The UV-Vis spectra of $3Zn(OH)_2 \cdot 2ZnCO_3$ and crotonic acid (CTA) (Fig. S3†) showed no obvious changes in $3Zn(OH)_2 \cdot 2ZnCO_3$ and CTA before and after irradiation for 2 h. Therefore, according to previous work, the photochromic process should be an electron-transfer process from CTA (electron donor) to 4,4′-bipy (electron acceptor). The nearest distances between the carboxylate oxygen atom and the nitrogen atom of the pyridinium ring were 3.0244(34) Å for **1** and 3.0761(32) Å for **2**. As these distances were almost identical, the influence of distance on electron transfer in the two compounds was not distinct. However, $\pi \cdots \pi$ stacking interactions between the pyridinium rings and CTA double bonds with their center-to-center distances of 3.5230(1) Å for **1** and 3.3624(2) Å for **2** showed that they might be more helpful for generating free radicals and electron transfer in **2**.

The time-dependent UV-Vis spectra data underwent linear fitting at 562 nm for **1** and 572 nm for **2** (Fig. 6) and illustrated that their photochromic behaviors followed first-order reaction kinetics, which can be explained using the following equation:

$$\ln(A_0 - A_\infty)/(A_t - A_\infty) = Kt$$

where K is the first-order reaction kinetics rate constant, and A_0, A_t, and A_∞ are the absorbances before irradiation, after irradiation for time t, and at the end of the reaction, respectively.[25,26] The fitting rate constants (K_{obs}) for compounds **1** and **2** were ~9.60×10^{-4} and 1.14×10^{-3} s^{-1}, respectively. According to the UV-Vis spectra, the conversion rate of these two complexes

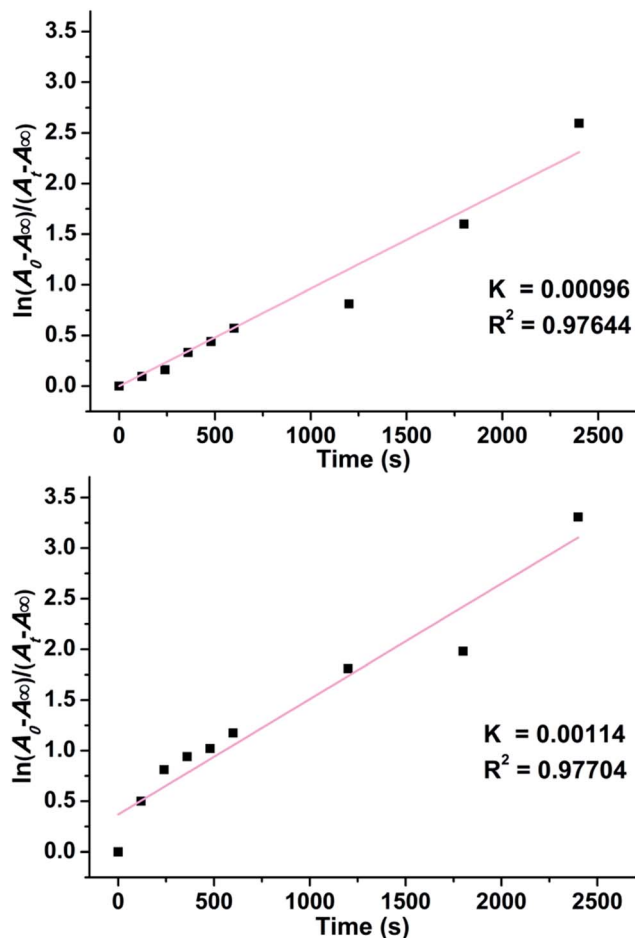Fig. 4 UV-Vis absorption spectra of **1** (top) and **2** (bottom), which are dependent on illumination under ambient conditions.

Fig. 6 First-order kinetics of photoinduced coloration process of **1** (top) and **2** (bottom) under ambient conditions.

Fig. 7 Time-dependent fluorescence spectra (λ_{ex} = 370 nm) of **1** (top) and **2** (bottom) under ambient conditions.

at the beginning was faster than at a later time. This phenomenon was caused by photochemical reactions occurring on surfaces initially and then inside in the final stages.[27] This showed that the coloration speed of **2** was faster than that of **1** in Fig. 6. Consequently, the $\pi\cdots\pi$ stacking interaction between the pyridinium ring and CTA double bond should be the main factor in the color of compound **2** changing faster than that of **1**.

Photoluminescence properties

The photochromic process is generally associated with a change in the fluorescence properties.[5,28–30] As shown in Fig. 7, compounds **1** and **2** had two broad emissive bands upon excitation with a 370 nm Xe light under ambient conditions, centered at 453 nm for **1** and 446 nm for **2**, respectively. BPY and CTA showed PL emission bands with peaks at 434 nm and 469 nm, respectively (Fig. S7†). By comparing the peak values of **1**, **2**, BPY, and CTA, the conclusion that the PL of **1** and **2** can be a preliminary definition due to the combination of emission from BPY and CTA can be obtained. The time-dependent PL spectra of **1** and **2** showed that the PL intensity decreased gradually with increasing irradiation time, reaching about 47.1% for **1** and 41.8% for **2** of the initial value after 120 min.
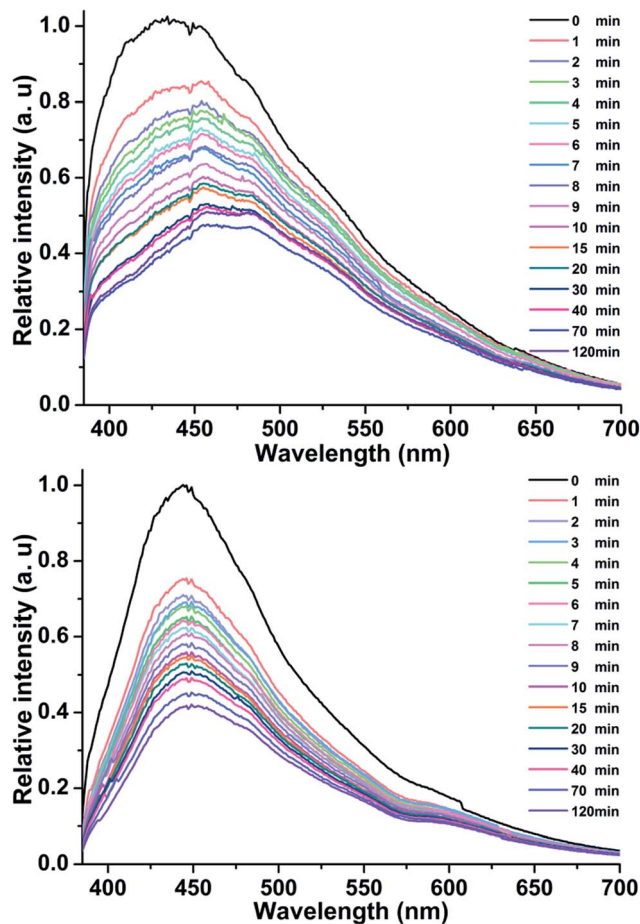
When the emission values did not change further with increasing irradiation time, the colors of compounds remained stable with extended irradiation times. Accordingly, the UV-Vis absorption data peaked. This further proved that PL quenching was also accompanied by the ET process. Such a phenomenon is common for compounds that can undergo ET photochromism. The different PL intensity decreases also corresponded with the coloration processes in **1** and **2**, which further supported that ET was significantly affected by $\pi\cdots\pi$ stacking interactions between the pyridinium ring and CTA double bond.

Conclusions

In summary, two new photochromic coordination compounds with non-photochromic ligands were prepared and characterized. This work proposed using multi-metal units as connections in photochromic coordination compounds with non-photochromic ligands, which has enriched this system. Meanwhile, the $\pi\cdots\pi$ interactions proved to be beneficial for electron transfer in these photochromic compounds. These results will aid the design and synthesis of new photochromic compounds with different multinuclear metal centers and high performance.

Acknowledgements

Notes and references

1 (a) Q. Wang and D. Ma, *Chem. Soc. Rev.*, 2010, **39**, 2387–2398; (b) G.-H. Alexis, U. Manuel, M. Dragos, T. Evgenii, S. Jutta, G. Lutz, B. David, S. Peter and H. Stefan, *J. Am. Chem. Soc.*, 2017, **139**, 335–341; (c) S. Lee, Y. You, K. Ohkubo, S. Fukuzumi and W. Nam, *Chem. Sci.*, 2014, **5**, 1463–1474; (d) P.-X. Li, M.-S. Wang, M.-J. Zhang, C.-S. Lin, L.-Z. Cai, S.-P. Guo and G.-C. Guo, *Angew. Chem., Int. Ed.*, 2014, **53**, 11529–11531.

2 (a) I. F. A. Mariz, F. Siopa, C. A. B. Rodrigues, C. A. M. Afonso, X. Chen, J. M. G. Martinho and E. M. S. Maçôas, *J. Mater. Chem. C*, 2015, **3**, 10775–10782; (b) Y.-J. Cui, Y.-F. Yue, G.-D. Qian and B.-L. Lin, *Chem. Rev.*, 2012, **112**, 1126–1162.

3 Z.-C. Hu, B. J. Deibert and J. Li, *Chem. Soc. Rev.*, 2014, **43**, 5815–5840.

4 K. K.-W. Lo, K. Y. Zhang, S.-K. Leung and M.-C. Tang, *Angew. Chem., Int. Ed.*, 2008, **47**, 2213–2216.

5 C.-J. Zhang, Z.-W. Chen, R.-G. Lin, M.-J. Zhang, P.-X. Li, M.-S. Wang and G.-C. Guo, *Inorg. Chem.*, 2014, **53**, 847–851.

6 Z.-Y. Fu, Y. Chen, J. Zhang and S.-J. Liao, *J. Mater. Chem.*, 2011, **21**, 7895–7897.

7 I. Stassen, N. Burtch, A. Talin, P. Falcaro, M. Allendorf and R. Ameloot, *Chem. Soc. Rev.*, 2017, **46**, 3185–3241.

8 T. Gong, X. Yang, J.-J. Fang, Q. Sui, F.-G. Xi and E.-Q. Gao, *ACS Appl. Mater. Interfaces*, 2017, **9**, 5503–5512.

9 K. Boopathy and P. Ramasamy, *J. Mol. Struct.*, 2015, **1080**, 37–43.

10 E. Pershagen and K. E. Borbas, *Coord. Chem. Rev.*, 2014, **273**, 30–46.

11 D.-P. Yan, H.-J. Yang, Q.-Y. Meng, H.-Y. Lin and M. Wei, *Adv. Funct. Mater.*, 2014, **24**, 587–594.

12 S. Saha, G. Das, J. Thote and R. Banerjee, *J. Am. Chem. Soc.*, 2014, **136**, 14845–14851.

13 (a) G. J. Kavarnos and N. J. Turro, *Chem. Rev.*, 1986, **86**, 401–449; (b) M. R. Wasielewski, *Chem. Rev.*, 1992, **92**, 435–461.

14 K. V. Rao, K. K. R. Datta, M. Eswaramoorthy and S. J. George, *Adv. Mater.*, 2013, **25**, 1713–1718.

15 (a) Q.-X. Yao, L. Pan, X.-H. Jin, J. Li, Z.-F. Ju and J. Zhang, *Chem.–Eur. J.*, 2009, **15**, 11890–11897; (b) Q.-X. Yao, Z.-F. Ju, X.-H. Jin and J. Zhang, *Inorg. Chem.*, 2009, **48**, 1266–1268; (c) X.-H. Jin, J.-K. Sun, X.-M. Xu, Z.-H. Li and J. Zhang, *Chem. Commun.*, 2010, **46**, 4695–4697.

16 M. D. Allendorf, C. A. Bauer, R. K. Bhakta and R. J. T. Houka, *Chem. Soc. Rev.*, 2009, **38**, 1330–1352.

17 J. Heine and K. Müller-Buschbaum, *Chem. Soc. Rev.*, 2013, **42**, 9232–9242.

18 CrystalClear, *version 1.35, Software User's Guide for the Rigaku R–Axis, and Mercury and Jupiter CCD Automated X–ray Imaging System, Rigaku Molecular Structure Corporation*, Utah, 2002.

19 SHELXTL Reference Manual, *version 5*, Siemens Energy & Automation Inc., Madison, WI, 1994.

20 J. Wang, S.-L. Li and X.-M. Zhang, *ACS Appl. Mater. Interfaces*, 2016, **8**, 24862–24869.

21 R. Li, S.-H. Wang, Z.-F. Liu, X.-X. Chen, Y. Xiao, F.-K. Zheng and G.-C. Guo, *Cryst. Growth Des.*, 2016, **16**, 3969–3975.

22 C. Janiak, *J. Chem. Soc., Dalton Trans.*, 2000, 3885–3896.

23 H.-T. Feng, J.-B. Xing, Y.-S. Zheng, B. Pan, C. Zhang, L. Wang and Y. Xie, *Chem. Mater.*, 2015, **27**, 7812–7819.

24 (a) Z.-Q. Liu, Y. Zhao, Y. Deng, X.-D. Zhang, Y.-S. Kang, Q.-Y. Lu and W.-Y. Sun, *Sens. Actuators, B*, 2017, **250**, 179–188; (b) Y.-L. Li, Y. Zhao, P. Wang, Y.-S. Kang, Q. Liu, X.-D. Zhang and W.-Y. Sun, *Inorg. Chem.*, 2016, **55**, 11821–11830; (c) Y. Deng, P. Wang, Y. Zhao, Y.-S. Kang and W.-Y. Sun, *Microporous Mesoporous Mater.*, 2016, **227**, 39–47.

25 R.-G. Lin, G. Xu, G. Lu, M.-S. Wang, P.-X. Li and G.-C. Guo, *Inorg. Chem.*, 2013, **52**, 1199–1205.

26 R.-G. Lin, G. Xu, G. Lu, M.-S. Wang, P.-X. Li and G.-C. Guo, *Inorg. Chem.*, 2014, **53**, 5538–5545.

27 M. Li, L.-J. Yuan and Z.-Y. Fu, *Inorg. Chem. Commun.*, 2015, **57**, 58–61.

28 S.-Q. Zhang, F.-L. Jiang, Y. Bu, M.-Y. Wu, J. Ma, X.-C. Shan, K.-C. Xiong and M.-C. Hong, *CrystEngComm*, 2012, **14**, 6394–6396.

29 Z.-F. Wu, B. Tan, J.-Y. Wang, C.-F. Du, Z.-H. Deng and X.-Y. Huang, *Chem. Commun.*, 2015, **51**, 157–160.

30 S.-H. Wang, F.-K. Zheng, M.-J. Zhang, Z.-F. Liu, J. Chen, Y. Xiao, A.-Q. Wu and G.-C. Guo, *Inorg. Chem.*, 2013, **52**, 10096–10104.